



Montréal, Québec
May 29 to June 1, 2013 / 29 mai au 1 juin 2013

Harmonic Response of Doubly symmetric Thin-walled Members based on the Vlasov Theory– I. Analytical Solution

Mohammed Ali Hjaji¹ and Magdi Mohareb²

¹ Department of Mechanical and Industrial Engineering, Tripoli University, Tripoli, Libya

² Department of civil engineering, University of Ottawa, Ottawa, Canada

Abstract: The steady state response of thin-walled members with doubly symmetric cross-sections subjected to harmonic forces is investigated. Using the Hamiltonian functional, the governing differential equations and related boundary conditions are formulated based on the Vlasov thin walled beam theory. The formulation takes into account the effect of warping deformation and translational and rotary inertia. The resulting governing field equations are then exactly solved and closed form solutions for transverse and torsional responses are obtained for common boundary conditions. Numerical examples are then presented and comparisons are made against other established Abaqus beam and shell solutions to assess the accuracy of the present analytical solutions.

1. Introduction and Background

Thin-walled members are used as structural components in aircraft wing and fuselage structures, vehicle axles, propellant and turbine blades, ship and marine structural frames, steel building structures. In these applications, members are commonly subjected to cyclic dynamic loading (e.g., harmonic forces). Sources of such forces include aerodynamic effects, hydro-dynamic wave motion and wind loading. Also, harmonic forces can be arise from unbalance in rotating machinery and propellants, reciprocating machines and traffic motion in steel bridge structures. In such applications, thin-walled members under effect of harmonic loads are prone to fatigue failure, an important limit state when designing these structural members. Under harmonic forces, the steady state component of the response is sustained for a long time and is thus of particular importance in fatigue design. In contrast, the transient component of response which is induced only at the beginning of the excitation tends to dampen out quickly and is thus of no importance in assessing the fatigue life of a detail. Within this context, the present study aims at developing an accurate and efficient solution which captures and isolates the steady state response. The present analytical solutions are also able to capture the static response and predict the eigen-frequencies and eigen-modes of the member.

2. Literature review

The classical theory of thin-walled beams developed by Vlasov (1961) is widely used in the analysis of thin-walled members with open sections. The theory is based on two kinematic assumptions; (i) the beam cross-section does not deform in its own plane, and (ii) the transverse shear strains at the mid-surface are negligible. Friberg (1983), Leung (1991,1992), Chen and Tamma (1994), Li et al. (2004) and Kim et al. (2007) developed the dynamic stiffness matrix of Vlasov beam in which the shear deformation is ignored. Using the normal mode method, Eslimy-Isfahany et al. (1996) developed a solution for the response of coupled bending-torsion vibration of thin-walled beams under deterministic and random excitations. Yaman (1997) studied the triply coupled forced vibration behaviour of thin-walled beams with open

channel cross-sections under single-point harmonic excitation by using the wave propagation approach. Adam (1999) analyzed the coupled bending-torsional vibrations. His analysis incorporates warping effects. Yaman (2002) developed an analytical solution for the triply coupled forced vibrations of elastically supported, open cross-section, single and multi-bay channels. A common feature between the solutions of Yaman (1997), Adam (1999), and Yaman (2002) is their solutions capture warping effects but omits shear deformation effects. Lee and Kim (2002a,b) investigated the free vibration of thin-walled composite beams with doubly symmetric and channel cross-sections. The influence of constant lateral forces on the bending-torsional coupled free vibration of thin-walled open members was lately studied by Voros (2008, 2009). Recently, Vo and Lee (2010) and Vo et al. (2011) studied the coupled flexural-torsional free vibration of thin-walled open composite beams under constant axial forces and end moments. For the most part, the above studies have focused on solutions primarily aimed at extracting the natural frequencies and mode shapes, with little or no attention on determining the response of members under harmonic forces.

To the best of the author's knowledge, closed-form solutions of thin-walled based on the Vlasov theory for open members subjected to harmonic forces have not been published. Within this context, this paper formulates the field equations and boundary conditions for the problem and provides closed form analytical solutions for members of doubly symmetric sections subjected to various harmonic excitations. The present solution captures warping effects as well as translational and rotational inertial effects.

3. Assumptions

The following assumptions are made:

1. The thin-walled member is linearly elastic and prismatic,
2. Strains and rotations are assumed small,
3. The member cross-section does not deform in its own plane, and
4. Shear strains on the middle-surface of the cross-section are negligible.

4. Kinematics and Displacements

A thin-walled member with doubly symmetric open cross-section is assumed to have has a fixed right-handed orthogonal Cartesian coordinate system (X, Y, Z) with the Z coinciding with the longitudinal axis. A local coordinate system (n, s, Z) is positioned on the contour (middle line of the cross-section) in which coordinates n and s are taken along the normal and along the tangent to the middle surface at the point of interest. Based on the above assumptions, the longitudinal displacement $w_p(z, s, t)$ and in-plane displacements $u_p(z, s, t)$ and $v_p(z, s, t)$ of a generic point $p(x, y)$ located on the middle surface of the doubly symmetric section (Fig. 1) are respectively given by [Vlasov 1961]

$$[1] \quad w_p(z, s, t) = w(z, t) - x(s)u'(z, t) - y(s)v'(z, t) - \omega(s)\theta'_z(z, t)$$

$$[2-3] \quad u_p(z, s, t) = u(z, t) - y(s)\theta_z(z, t), \quad v_p(z, s, t) = v(z, t) + x(s)\theta_z(z, t)$$

in which $w(z, t)$ is an integration function which represents the average longitudinal displacement, $u(z, t)$ and $v(z, t)$ are the displacement components of the shear centre S_c along the principal directions X and Y respectively, $\theta_z(z, t)$ is the angle of twist, $x(s)$ and $y(s)$ are the coordinates of point p along the principal axes (Fig. 1a), and $\omega(s)$ is the warping function (Vlasov 1961) of the cross-section defined by $\omega(s) = \int_A h(s) dA$. All primes denote derivatives with respect to coordinate z .

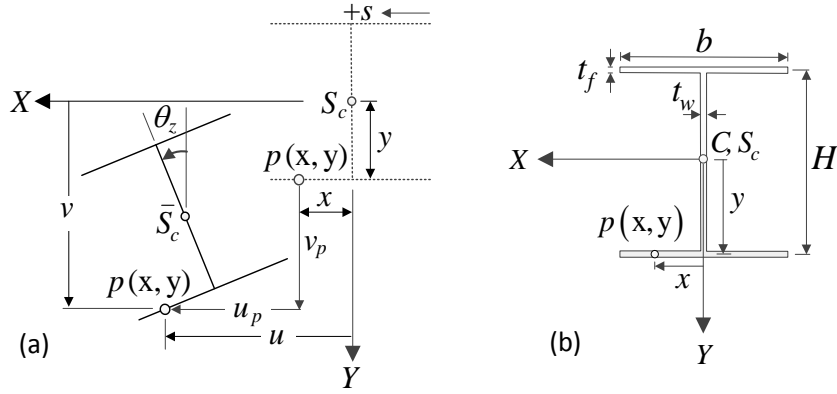


Figure (1): Coordinate systems and displacement components

5. Expressions for Force Functions

The thin-walled member is assumed to be subjected to (i) general distributed harmonic loads within the structural member and (ii) concentrated harmonic loads at both ends, i.e.,

$$[4] \quad q_z(z, t), q_x(z, t), q_y(z, t), m_z(z, t) = [\bar{q}_z(z), \bar{q}_x(z), \bar{q}_y(z), \bar{m}_z(z)] e^{i\Omega t}$$

$$[5] \quad N_z(z_e, t), V_x(z_e, t), V_y(z_e, t), M_z(z_e, t), M_x(z_e, t), M_y(z_e, t), M_w(z_e, t) \\ = [\bar{N}_z(z_e), \bar{V}_x(z_e), \bar{V}_y(z_e), \bar{M}_z(z_e), \bar{M}_x(z_e), \bar{M}_y(z_e), \bar{M}_w(z_e)] e^{i\Omega t}$$

where Ω is the circular exciting frequency of the external forces, $i = \sqrt{-1}$ is the imaginary constant $q_z(z, t), q_x(z, t), q_y(z, t)$ are the distributed longitudinal, transverse and lateral harmonic forces, $m_z(z, t)$ is the distributed harmonic torsion, $N_z(z_e, t), V_x(z_e, t), V_y(z_e, t)$ are the concentrated longitudinal, transverse and lateral harmonic forces, $M_z(z_e, t), M_x(z_e, t), M_y(z_e, t)$ are the harmonic end moments and $M_w(z_e, t)$ is the harmonic end bimoments, all forces and moments applied at beam ends ($z_e = 0, \ell$). All applied forces are assumed to have the same sign convention as those of the end displacements (Figure 1).

6. Expressions for Displacement Fields

In the absence of damping and under the above harmonic forces, the steady state displacements at the middle surface are assumed to take the harmonic form

$$[6] \quad w(z, t), u(z, t), v(z, t), \theta_z(z, t) \approx [\bar{w}(z), \bar{u}(z), \bar{v}(z), \bar{\theta}_z(z)] e^{i\Omega t}$$

in which $\bar{w}(z), \bar{u}(z), \bar{v}(z), \bar{\theta}_z(z)$ are space functions for longitudinal translation, bending translations and angle of twist, respectively. In line with the objective of the paper, the displacement functions proposed in Equation (9) neglect the transient component of the response.

6. Variational Formulation

The variational form of the Hamiltonian functional δH is taken to be stationary, i.e.,

$$[7] \quad \delta H = \int_{t_1}^{t_2} (\delta T - \delta U + \delta W) dt = 0$$

in which δT is the variation of kinetic energy, δU is the variation of internal strain energy and δW is the virtual work done by external forces, and the integration is performed between arbitrary time limits t_1 and t_2 . The expressions of the variations are

$$[8-9] \quad \delta T = \int_0^\ell \int_A \rho [\dot{u}_p \delta \dot{u}_p + \dot{v}_p \delta \dot{v}_p + \dot{w}_p \delta \dot{w}_p] dA dz, \quad \delta U = \int_0^\ell \int_A E \varepsilon_{zz} \delta \varepsilon_{zz} dA dz + \int_0^\ell GJ \theta'_z \delta \theta'_z dz$$

$$[10] \quad \delta W = [N_z(z_e, t) \delta w(z_e, t)]_0^\ell + [V_x(z_e, t) \delta u(z_e, t)]_0^\ell + [V_y(z_e, t) \delta w(z_e, t)]_0^\ell$$

$$+ [M_x(z_e, t) \delta v'(z_e, t)]_0^\ell + [M_y(z_e, t) \delta u'(z_e, t)]_0^\ell + [M_z(z_e, t) \delta \theta_z(z_e, t)]_0^\ell$$

$$+ [M_w(z_e, t) \delta \theta'_z(z_e, t)]_0^\ell + \int_0^\ell [q_z(z, t) \delta w(z, t) + q_x(z, t) \delta u(z, t)$$

$$+ q_y(z, t) \delta v(z, t) + m_z(z, t) \delta \theta_z(z, t)] dz$$

where E is the modulus of elasticity, G is the shear modulus, ρ is the density of member material, ε_{zz} is the longitudinal strain taken as $\varepsilon_{zz} \approx \partial w_p / \partial z$, J is the Saint-Venant torsional constant, A is the cross-sectional area. All primes denote derivatives with respect to space coordinate z , while dots denote derivatives with respect to time t .

7. Field Equations

From Equations (1-3) and (4-6), by substituting into equations (8-10), and the resulting energy expressions into Equation (7), performing integration by parts and enforcing the orthogonality conditions $\int_A [x(s), y(s), x(s)y(s), x(s)\omega(s), y(s)\omega(s), \omega(s)] dA = 0$, the equations of motion are recovered:

$$[11-12] \quad EA \bar{w}'' + \rho A \Omega^2 \bar{w} = \bar{q}_z(z), \quad EI_{yy} \bar{u}^{iv} + \rho \Omega^2 I_{yy} \bar{u}'' - \rho A \Omega^2 \bar{u} = \bar{q}_x(z)$$

$$[13-14] \quad EI_{xx} \bar{v}^{iv} + \rho \Omega^2 I_{xx} \bar{v}'' - \rho A \Omega^2 \bar{v} = \bar{q}_y(z), \quad EC_w \bar{\theta}_z^{iv} + (\rho \Omega^2 C_w - GJ) \bar{\theta}_z'' - \rho A \Omega^2 r_o^2 \bar{\theta}_z = \bar{m}_z(z)$$

It is noted that, the above governing differential equations are similar to those derived by Vlasov (1961) for free vibration of thin-walled beams with three differences: (a) The time dependence of the equations for motion has been eliminated as direct outcome of the substitution made in Eq. (6), (b) the presence of non-zero forcing functions on the right hand sides of Equations (11-14), and (c) the inertia terms are now specialized for the case of harmonic forces. It is observed that the four equations of motion are uncoupled for the case of doubly-symmetric cross-sections considered in the present study. The associated natural and essential boundary conditions are:

$$[EA \bar{w}' - \bar{N}_z(z)] \delta \bar{w}(z) \Big|_0^\ell = 0, [EI_{yy} \bar{u}'' - \bar{M}_y(z)] \delta \bar{u}'(z) \Big|_0^\ell = 0, [EI_{yy} \bar{u}''' - \bar{V}_x(z)] \delta \bar{u}(z) \Big|_0^\ell = 0$$

$$[EI_{xx} \bar{v}'' - \bar{M}_x(z)] \delta \bar{v}'(z) \Big|_0^\ell = 0, [EI_{xx} \bar{v}''' - \bar{V}_y(z)] \delta \bar{v}(z) \Big|_0^\ell = 0$$

$$[15-21] \quad \left[EC_w \bar{\theta}_z''' - GJ \bar{\theta}_z' - \bar{M}_z(z) \right] \delta \bar{\theta}_z(z) \Big|_0^\ell = 0, \quad \left[EC_w \bar{\theta}_z'' - \bar{M}_w(z) \right] \delta \bar{\theta}_z'(z) \Big|_0^\ell = 0$$

In the following, focus will be on the solution of bending and torsional equations (i.e., Eqs. 12-14).

8. Homogeneous Solutions for Bending and Torsional Equations

The homogeneous solutions for lateral, transverse and torsional equations (12-14) are obtained by setting the right hand side to zero, i.e., $\bar{q}_x(z) = \bar{q}_y(z) = \bar{q}_z(z) = 0$. The homogeneous solutions $\bar{u}_h(z)$, $\bar{v}_h(z)$ and $\bar{\theta}_{zh}(z)$ are assumed to take the form

$$[22] \quad \bar{u}_h(z) = A_i e^{\alpha_i z}, \quad \bar{v}_h(z) = B_i e^{\beta_i z}, \quad \bar{\theta}_{zh}(z) = C_i e^{\gamma_i z}, \quad \text{for } i = 1, 2, 3, 4$$

where A_i, B_i and C_i (for $i = 1, 2, 3, 4$) represent three sets of independent unknown integration constants to be determined from the boundary conditions of the problem. Equations (22) are substituted into Equations (12-14) and the resulting three characteristic equations are solved for constants yielding the roots $\beta_{1,2} = \pm \left[-q_1 + (q_2)^{1/2} \right]^{1/2}$, $\beta_{3,4} = \pm i \left[q_1 + (q_2)^{1/2} \right]^{1/2}$, where $q_1 = \rho \Omega^2 / 2E$, $q_2 = q_1^2 - (\rho A / EI_{yy})$. The roots α_i are obtained through similar expression after replacing I_{yy} by I_{xx} . The roots γ_i are obtained by $\gamma_{1,2} = \pm \left[-s_1 + (s_2)^{1/2} \right]^{1/2}$, $\gamma_{3,4} = \pm i \left[s_1 + (s_2)^{1/2} \right]^{1/2}$, where $s_1 = (\rho \Omega^2 C_w - GJ) / 2EC_w$ and $s_2 = \rho A \Omega^2 r_o^2 / EC_w$.

9. General Solutions for Bending and Torsional Equations

The general solution for the case of constant forces $\bar{q}_x, \bar{q}_y, \bar{m}_z$ are obtained by summing the homogeneous and particular solutions, yielding

$$[23-24] \quad \bar{u}(z) = \langle E_\alpha(z) \rangle_{1 \times 4}^T \{A_i\}_{4 \times 1} + (\bar{q}_x / \rho A \Omega^2), \quad \bar{v}(z) = \langle E_\beta(z) \rangle_{1 \times 4}^T \{B_i\}_{4 \times 1} + (\bar{q}_y / \rho A \Omega^2),$$

$$[25] \quad \bar{\theta}_z(z) = \langle E_\gamma(z) \rangle_{1 \times 4}^T \{C_i\}_{4 \times 1} + (-\bar{m}_z / \rho A \Omega^2 r_o^2)$$

in which $\langle E_r(z) \rangle_{1 \times 4}^T = \langle e^{r_1 \ell} \mid e^{r_2 \ell} \mid e^{r_3 \ell} \mid e^{r_4 \ell} \rangle_{1 \times 4}^T$, for $(r = \alpha, \beta, \gamma)$.

9.1 Case 1: Cantilever beam under transverse forces

A cantilever I-beam subjected to a transverse harmonic force $\bar{P}_y(\ell) e^{i\Omega t}$ and bending moment $\bar{M}_x(\ell) e^{i\Omega t}$ at the free end is considered. Imposing the related boundary conditions $\delta \bar{v}(0) = \delta \bar{v}'(0) = 0$, $EI_{xx} \bar{v}'''(\ell) = \bar{P}_y(\ell)$ and $EI_{xx} \bar{v}''(\ell) = \bar{M}_x(\ell)$, the general solution is

$$[26] \quad \bar{v}(z) = \langle E_\beta(z) \rangle_{1 \times 4}^T \left[\Phi_\beta \right]_{4 \times 4}^{-1} \{Q_\beta\}_{4 \times 1} + (\bar{q}_y / \rho A \Omega^2)$$

$$\text{where } \langle \mathbf{Q}_\beta \rangle_{1 \times 4}^T = \left\langle 0 \mid 0 \mid \frac{\bar{P}_y(\ell)}{EI_{xx}} \mid \frac{M_x(\ell)}{EI_{xx}} \right\rangle_{1 \times 4}^T, \quad [\Phi_\beta]_{4 \times 4} = \begin{bmatrix} 1 & 1 & 1 & 1 \\ \beta_1 & \beta_2 & \beta_3 & \beta_4 \\ \beta_1^3 e^{\beta_1 \ell} & \beta_2^3 e^{\beta_2 \ell} & \beta_3^3 e^{\beta_3 \ell} & \beta_4^3 e^{\beta_4 \ell} \\ \beta_1^2 e^{\beta_1 \ell} & \beta_2^2 e^{\beta_2 \ell} & \beta_3^2 e^{\beta_3 \ell} & \beta_4^2 e^{\beta_4 \ell} \end{bmatrix}_{4 \times 4}.$$

9.2 Case 2: Solution for Simply-supported beam under twist

A given simply-supported I-beam is subjected to (i) distributed harmonic torsion $\bar{m}_z(z)e^{i\Omega t}$, bimoment $\bar{m}_w(z)e^{i\Omega t}$, and (ii) concentrated bimoment $\bar{M}_w(z_e)e^{i\Omega t}$ applied at both ends (i.e., $z_e=0, \ell$). The beam supports leaves the end sections free to warp and to rotate about X and Y axes. By imposing the boundary conditions at beam both ends; $\delta\bar{\theta}_z(0)=0$, $EC_w\bar{\theta}_z''(0)=-\bar{M}_w(0)$, $\delta\bar{\theta}_z(\ell)=0$ and $EC_w\bar{\theta}_z''(\ell)=\bar{M}_w(\ell)$, the total closed-form steady state solution for simply-supported beam under harmonic torsional loading is then obtained by

$$[27] \quad \bar{\theta}_z(z) = \langle E_\gamma(z) \rangle_{1 \times 4}^T [\Phi_\gamma]_{4 \times 4}^{-1} \{Q_\gamma\}_{4 \times 1} + (-\bar{m}_z / \rho A \Omega^2 r_o^2), \quad \text{for } 0 \leq z \leq \ell/2$$

$$\text{where } [\Phi_\gamma]_{4 \times 4} = \begin{bmatrix} 1 & 1 & 1 & 1 \\ \gamma_1^2 & \gamma_2^2 & \gamma_3^2 & \gamma_4^2 \\ e^{\gamma_1 \ell} & e^{\gamma_2 \ell} & e^{\gamma_3 \ell} & e^{\gamma_4 \ell} \\ \gamma_1^2 e^{\gamma_1 \ell} & \gamma_2^2 e^{\gamma_2 \ell} & \gamma_3^2 e^{\gamma_3 \ell} & \gamma_4^2 e^{\gamma_4 \ell} \end{bmatrix}_{4 \times 4}, \quad \text{and } \{Q_\gamma\}_{4 \times 1} = \begin{Bmatrix} \bar{m}_z / \rho A \Omega^2 r_o^2 \\ -\bar{M}_w(0) / EC_w \\ \bar{m}_z / \rho A \Omega^2 r_o^2 \\ \bar{M}_w(\ell) / EC_w \end{Bmatrix}_{4 \times 1}.$$

10. Numerical Examples and Discussion

The analytical closed-form solutions developed in the present study are used to provide the steady state dynamic response of thin-walled members under general harmonic excitations. The static response under harmonic forces can be approached by using very low exciting frequency $\Omega \approx 0.01\omega_1$ compared to the first natural frequency ω_1 . Two examples are conducted for beams with doubly symmetric cross-sections. In both examples, the material is assumed to be steel with $E=200GPa$, $G=77GPa$ and $\rho=7850Kg/m^3$, while the geometric properties are; total height $d=252mm$, flange width $b=203mm$, flange thickness $t_f=13.5mm$, web thickness $t_w=8.0mm$, $A=7389mm^2$, $I_{xx}=87.3 \times 10^6 mm^4$, $J=374 \times 10^3 mm^4$, $C_w=268 \times 10^9 mm^6$. Results based on the present formulations are compared with Abaqus shell and beam solution. In Abaqus shell model, a shell S4R element with six degrees of freedom per node (i.e., three translations and three rotations) is used. The element captures shear deformation and distortional effects, while in the case of Abaqus beam model, a two-noded B31OS beam element with seven degrees of freedom per node (i.e., three translation, three rotations and warping deformation) which captures the shear deformation effects due to bending but discounts shear deformation effect due to warping and distortional effects.

10.1 Example (1) –Simply-supported Beam under Distributed Harmonic Forces

A 5.0m span simply-supported beam of doubly symmetric I-section subjected to uniformly distributed harmonic forces (1) twisting moment $m_z(z,t)=1.20e^{i\Omega t} kNm/m$, and (2) transverse force $q_y(z,t)=8.0e^{i\Omega t} kNm/m$ is considered. Two values of exciting frequencies are used; (i) $\Omega=0.01\omega_1$ to capture the static response and (ii) $\Omega=1.25\omega_1$ to determine the steady state dynamic response of the beam. The first natural frequency for the given beam is $\omega_1=16.03Hz$. It is required to (i) conduct a steady state analysis and extract the transverse and torsional natural frequencies, (ii) conduct a quasi-static analysis by adopting an exciting frequency $\Omega\approx 0.01\omega_1$, and (iii) determine the steady state dynamic response $\Omega\approx 1.25\omega_1$.

In Abaqus shell model solution, a total of 6,000 S4R shell elements are used (i.e., 10 elements along each flange, 10 elements along the web height and 200 elements along the longitudinal axis of the beam), while in the case of Abaqus beam model, two hundred beam B31OS elements are needed to eliminate discretization errors.

10.1.1 Extracting of Natural Frequencies

The steady state analyses of the simply-supported I-beam under the given distributed harmonic torsion $m_z(z,t)=1.20e^{i\Omega t} kNm/m$ and transverse force $q_y(z,t)=8.0e^{i\Omega t} kNm/m$ are independently solved in order to extract the related torsional and transverse natural frequencies of the beam. The first three Natural frequencies extracted from the torsional and transverse steady state responses presented in Table (1) are conducted based on the present solution (i.e., Eqs. 31 and 32), Abaqus shell and beam models solutions. As a general observation, excellent agreement is observed between all three solutions for torsional natural frequencies, while for the case of transverse natural frequencies, the frequencies predicted by the present Vlasov formulation are the highest followed by the Abaqus B31OS beam model, while the natural frequencies predicted from Abaqus shell solution are the lowest. This is due to the fact that the present formulation provides the stiffest representation of the stiffness.

Table (1): Torsional and bending natural frequencies for Simply-supported I-beam

Mode	Abaqus shell solution [1]	Abaqus beam solution [2]	Present solution [3]	Difference = [1-2]/1	Difference = [1-3]/1
1 st Torsional	24.04	24.49	24.51	-1.87%	-1.96%
2 nd Torsional	72.43	73.51	73.58	-1.49%	-1.59%
3 rd Torsional	149.4	152.1	153.4	-1.81%	-2.68%
1 st Transverse	33.53	34.13	34.33	-1.79%	-2.39%
2 nd Transverse	125.5	133.3	134.8	-6.22%	-7.41%
3 rd Transverse	259.3	278.2	282.5	-7.29%	-8.95%

In contrast, the Abaqus shell solution which captures shear deformation and distortional effects provides the most flexible representation of the stiffness. The torsional and transverse frequencies predicted by Abaqus shell model differ from those based on the present Vlasov solution by 1.59%-2.68% for torsional modes and 2.39%-8.95% for transverse modes.

10.1.2 Static Transverse and Torsional Responses

Based on the present formulations (Equations 31 and 32), the static responses of the simply-supported I-beam under given harmonic distributed twisting moment and distributed transverse force with very low

exciting frequency $\Omega \approx 0.01\omega_1$ is approached. The static results for the maximum torsional rotation $\bar{\theta}_{z \max}$ and maximum transverse displacement \bar{v}_{\max} at the mid-span of the beam are presented in Table (2). It is noted that, results for torsional angle $\bar{\theta}_z(z)$ and transverse displacement $\bar{v}(z)$ based on the present Vlasov solution match nearly exactly those of the Abaqus beam model. Both solutions slightly vary from the Abaqus shell model solution. The differences are attributed to distortional effects of the section and shear deformation due to warping which are captured in shell model but not in the other two solutions.

10.1.3 Dynamic Transverse and Torsional Responses

Under uniformly distributed harmonic twisting moment $m_z(z,t) = 1.20e^{i\Omega t} \text{ kNm/m}$ and distributed transverse force $q_y(z,t) = 8.0e^{i\Omega t} \text{ kNm/m}$ with exciting frequency $\Omega = 1.25\omega_1 \approx 125.9 \text{ rad/sec}$, the maximum amplitudes of steady state torsional $\bar{\theta}_{z \max}$ and transverse \bar{v}_{\max} responses for the simply-supported I-beam are provided in Table (2).

Table (2): Torsional and transverse responses results for simply-supported I-beam

Variable	Type of Response	Abaqus Shell Solution[1]	Abaqus Beam Solution[2]	Present Solution[3]	Difference = [1-2]/1	Difference = [1-3]/1
$\bar{\theta}_{z \max}$ (rad)	Static $\Omega \approx 0.001\omega_1$	0.0803	0.0771	0.0769	3.99%	4.23%
$\bar{\theta}_{z \max}$ (rad)	Steady state $\Omega = 1.25\omega_1$	0.2476	0.2387	0.2371	3.59%	4.24%
\bar{v}_{\max} (mm)	Static $\Omega \approx 0.001\omega_1$	3.880	3.767	3.742	2.91%	3.56%
\bar{v}_{\max} (mm)	Steady state $\Omega = 1.25\omega_1$	-6.053	-5.871	-5.749	3.01%	5.02%

Figures (2a) and (2b) illustrate the steady state torsional $\bar{\theta}_z(z)$ and transverse $\bar{v}(z)$ responses along the beam span, respectively. Results are based on the solution developed in the present study, Abaqus shell and beam solutions. It is observed that, the torsional angle and transverse displacement results presented in tabular and graphical forms based on the present solution coincide with Abaqus beam element, but slightly differ from the shell solution which exhibits a slightly more flexible response. Again, the differences are attributed to cross-sectional distortional effects and shear deformation due to warping.

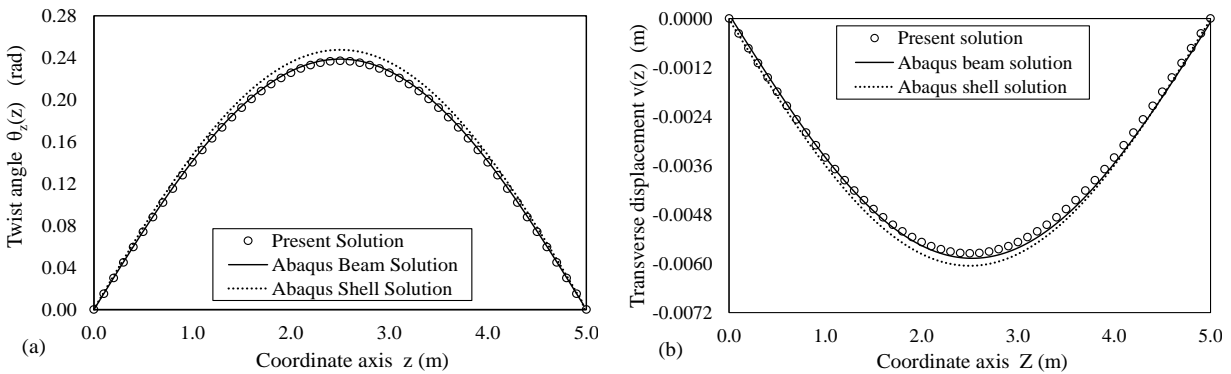


Figure (2): Static and Steady state responses for simply-supported I-beam

10.2 Example 2 - Cantilever I-beam under Concentrated harmonic Loads

A 3.0m span cantilever with the same doubly-symmetric cross-section as that given in Example 1 is subjected to two concentrated harmonic loads; (i) transverse load $P_y(\ell, t) = 18.0e^{i\Omega t}$ kN and (ii) twisting moment $M_z(\ell, t) = 2.80e^{i\Omega t}$ kNm applied at the free end of the cantilever beam. In order to validate the accuracy and exactness of the present analytical closed-form solutions, Abaqus shell and beam solutions are presented. It is required to (i) conduct a steady state dynamic response $\Omega \approx 1.28\omega_1$, where the first natural frequency related to transverse response of the cantilever is $\omega_1 = 34.33\text{Hz}$ and that related to the torsional response is $\omega_{t1} = 25.65\text{Hz}$, and (ii) extract the natural frequencies and steady state bending and torsional modes. Abaqus model solutions based on B31OS beam and S4R shell elements are presented for comparison.

10.2.1 Dynamic Response

For the exciting frequency $\Omega \approx 1.28\omega_1 \approx 125.4\text{rad/sec}$, Figures (3a, b) depict the transverse response $\bar{v}(z)$ and torsional response $\bar{\theta}_z(z)$ of the cantilever I-beam under concentrated harmonic transverse and torsional loads. Results are in excellent agreement with the Abaqus B31OS beam model (based on 200 elements) but slightly differ from Abaqus S4R shell solution (based on 2000 elements) which exhibits a little more flexible response. The present study predicts the maximum transverse displacement and twist angle are respectively 4.53% and 7.49% lower than those based on the Abaqus shell element model. Again, the differences are attributed to the distortional effect. It is noted that the distortional effects were observed to be more significant in torsional modes than in the bending modes.

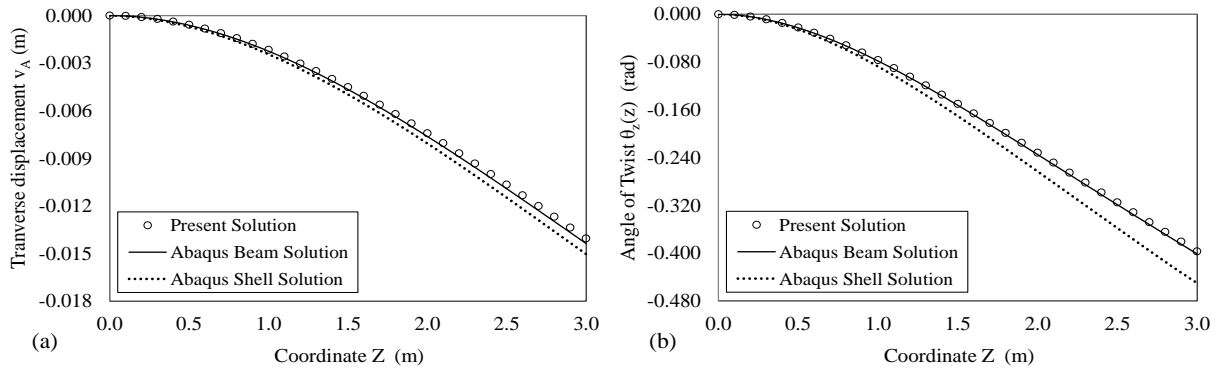


Figure (3): Steady state responses of cantilever I-beam under concentrated harmonic loads

10.2.2 Steady state bending and torsional responses

Under the given harmonic forces, the first three natural frequencies related to the bending and torsional responses can be extracted from the steady state transverse and torsional analyses as illustrated in Figures (1a) and (1c). Figures (1a) and (1c) demonstrate the peak transverse displacement and torsional angle at the cantilever tip as a function of exciting frequency. The exciting frequency is varied from nearly zero to 650Hz. Results based on the present Vlasov and Abaqus B31OS beam element solutions (which capture only the shear deformation due to bending) are provided for comparison. Both solutions closely predict the location of the first peak corresponding to the fundamental bending and torsional frequencies. For higher frequencies, some discrepancy in the location of the peak responses becomes apparent between the two solutions. It can be seen that the shear deformation captured by Abaqus beam model

make the resonance (peak) frequencies lower than those predicted by present solution. This is expected that the shear deformation effects are more significant for higher frequencies than the lower ones. The dynamic analyses of the steady state transverse and torsional responses of cantilever I-beam are illustrated in Figures (4b) and (4d), respectively, for different values of frequency ratios Ω_i/ω_1 , i.e., applied load frequency Ω_i to the first natural frequency ω_1 . Figure (4b) presents the transverse response of the cantilever I-beam subjected to the given transverse force for four values of frequency ratios $\Omega_1/\omega_1=0.5$, $\Omega_1/\omega_1=2.5$, $\Omega_1/\omega_1=6.5$ and $\Omega_1/\omega_1=17.5$ which are indicated on curves by numbers 1,2,3 and 4 (where $\omega_1=34.33Hz$ is the first natural transverse frequency of the beam), while the torsional response of the cantilever under concentrated harmonic torsion is illustrated using similar graphs in Figure (4d) for four values of exciting frequencies $\Omega_1=1.5\omega_{t1}$, $\Omega_1=6.5\omega_{t1}$, $\Omega_1=11.5\omega_{t1}$, and $\Omega_1=21.5\omega_{t1}$, where $\omega_{t1}=25.65Hz$ is the first natural torsional frequency.

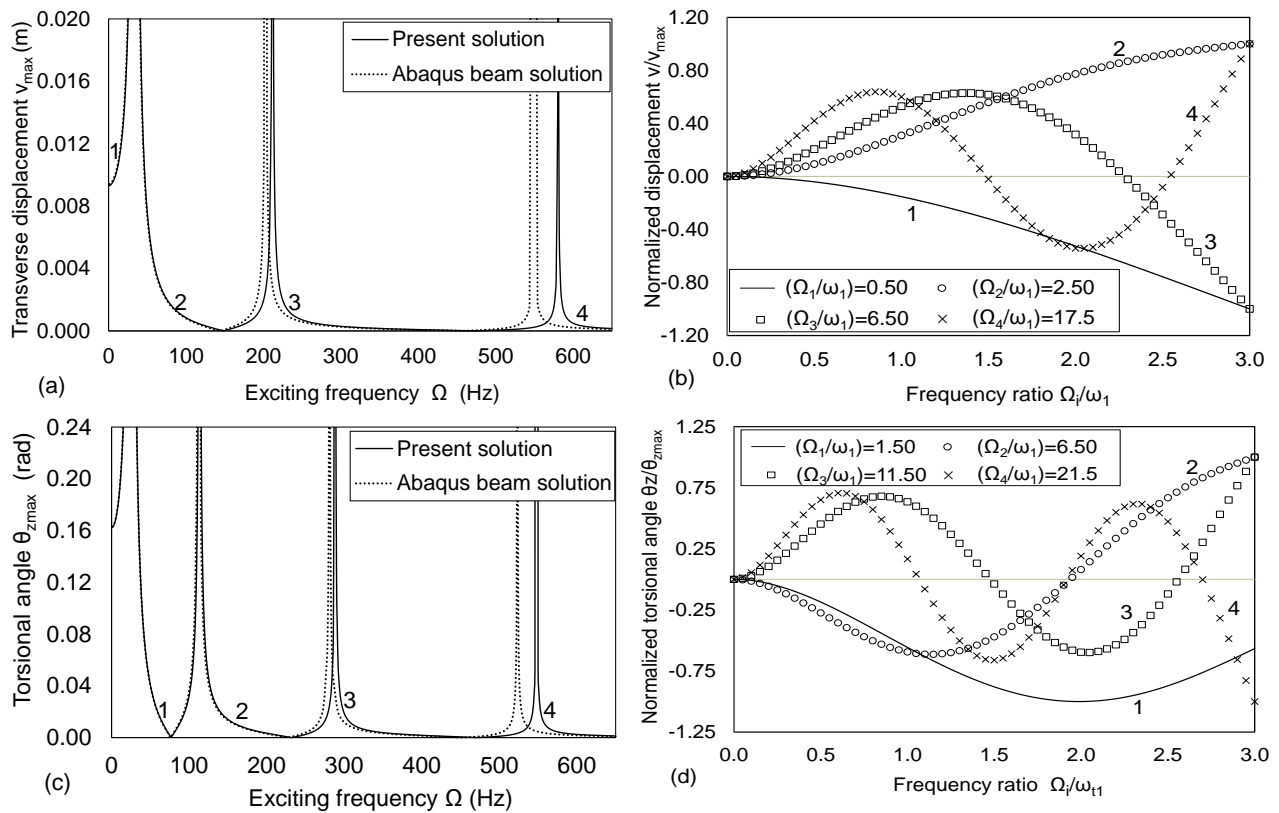


Figure (4): Bending and torsional responses of cantilever I-beam under concentrated harmonic forces

11. Conclusions

Based on the variational form of the Hamilton principle, the dynamic equations of motion and related boundary conditions for doubly-symmetric thin-walled members subjected to general harmonic forces were derived. Exact expressions for the analytical closed-form solutions for transverse and torsional responses are derived for doubly symmetric cantilever and simply-supported beams. Comparison with established Abaqus beam and shell solutions exhibits the validity and exactness of the present analytical solutions. The closed form solution developed in the present study will be used to develop exact shape functions for the problem and a super-convergent finite element in the companion paper (Hjaji and Mohareb 2013b).

12. References

- Adam, C. 1999, Forced vibrations of elastic bending-torsion coupled beams, *Journal of Sound and Vibration*, 221: 273-287.
- Chen, X. and Tamma, K. 1994, Dynamic response of elastic thin-walled structures influenced by coupling effects, *Computers and Structures*, 51(1): 91-105.
- Eslimy-Isfahany S. H. Banerjee J. R. 1996, Response of bending-torsion coupled beam to deterministic and random loads, *J. of Sound and vibration*, 195(2): 267-283.
- Friberg, P.O. 1983, Coupled vibration of beams-An exact dynamic element stiffness matrix, *International Journal for numerical methods in engineering*, 19: 479-493.
- Hjaji, M. A. and Mohareb, M. 2013b, Harmonic Response of Doubly symmetric Thin-walled Members based on the Vlasov Theory– II. Finite element formulation, CSCE 2013, 3rd Specialty Conference on Engineering Mechanics and Materials, Montreal, Canada.
- Kim, N. et al. 2007, Stiffness matrices for flexural-torsional/lateral buckling and vibration analysis of thin-walled beam, *Journal of Sound and Vibration*, 299: 739-756.
- Lee, J. and Kim, S. E. 2002, Free Vibration of Thin-walled Composite Beams with I-Shaped cross-sections, *Composite Structures*, 55(2): 205-215.
- Leung, A.Y.T. 1991, Natural shape functions of a compressed Vlasov element, *Thin-walled structures*, 11: 431-438.
- Leung, A.Y. 1992, Dynamic stiffness analysis of thin-walled structures, *Thin-walled structures*, 14: 209-22.
- Li, Jun et al. 2004, Dynamic response of axially loaded monosymmetrical thin-walled Bernoulli-Euler beams, *Thin-walled Structures*, 42(12): 1689-1707.
- Vlasov, V. 1961, *Thin-walled elastic beams*, second edition, Jerusalem, Israel Prog. for Scientific Translation.
- Voros, G. 2008, On Coupled Vibrations of Beams with Lateral Loads, *Journal of computational and Applied Mechanics*, 9 (2): 1-14.
- Voros, G. M. 2009, On Coupled bending-torsional vibrations of beams with initial loads, *Mechanics Research Communications*, 36: 603-611.
- Vo, T. P. and Lee, J. 2010, Interaction curves for vibration and buckling of thin-walled composite box beams under axial loads and end moments, *Applied Mathematical Modelling*, 34: 3142-3157.
- Vo, T. P. et al. 2011, Vibration analysis of thin-walled composite beams with I-shaped cross-sections, *Composite Structures*, 2011: 93(3-4): 812-820.
- Yaman, Y. 1997, Vibrations of open-section channels: a coupled flexural and torsional wave analysis, *Journal of Sound and Vibration*, 204(1): 131-158.
- Yaman, Y. 2002, Forced vibrations of triply coupled, periodically and elastically supported, finite, open-section channels, *Journal of Sound and Structures*, 250(4): 649-673.